An Improved Heap-Based Optimizer for Optimal Reactive Power Dispatch

SALAH K. ELSAYED [ID]1, **SALAH KAMEL** [ID]2, **ALI SELIM** [ID]2,
AND MAHROUS AHMED [ID]1, (Senior Member, IEEE)
[1]Department of Electrical Engineering, College of Engineering, Taif University, Taif 21944, Saudi Arabia
[2]Electrical Engineering Department, Faculty of Engineering, Aswan University, Aswan 81542, Egypt

Corresponding authors: Salah K. Elsayed (salah_kamal1982@yahoo.com), Salah Kamel (skamel@aswu.edu.eg), and Mahrous Ahmed
(m.elsamman@tu.edu.sa)

ABSTRACT Optimal reactive power dispatch (ORPD) in a typical power system is a complicated multi-objective optimization problem. The proper modeling of the multi-objective optimization problem has a significant impact on system operation and control. In this paper, an Improved Heap-based optimizer (IHBO) is proposed to improve the performance of a recently published technique called Heap-based optimizer (HBO). In addition, two algorithms based on the original HBO and IHBO are developed for solving OPRD problem. Pareto front approach is utilized in the proposed OPRD algorithm with the aim of solving two or three objective functions simultaneously. The performance of HBO is improved by utilizing the chaotic sequences with the aim of improving its global search capability and avoiding getting stuck in a local optimum. Both original HBO and proposed IHBO are applied to determine the optimal settings of the generator's voltages, shunt capacitor reactive power, and tap settings of transformers. Therefore, this study aims for minimizing three most objective functions of the real power loss, total voltage deviation (TVD) and voltage stability index (VSI), with satisfying different operational constraints. The effectiveness of the IHBO is tested on three test systems IEEE 30-bus, IEEE 57-bus, and IEEE 118-bus test systems. The results of the proposed IHBO are compared with recently published algorithms in the literature. The simulation results proven the superiority and robustness of IHBO in solving the ORPD problem.

INDEX TERMS Reactive power dispatch, optimization, heap-based optimizer, chaotic sequence.

I. INTRODUCTION

Nowadays, the existing power systems are imperative to operate at entire capacity due to the imbalance investment in power generation, transmission, and distribution sectors. Often, due to the aforementioned situation the heavy current flows in whole system tend to incur more losses and threatening power system stability. At last, this may lead to the risk of electricity interruptions in whole system of various severity levels. Hence, there is unanimity amongst the system operators to enhance the existing transmission and distribution systems through installation of power grid stations and new lines to make the system more smart, efficient, and reliable [1]. To subtend the mentioned challenges,

The associate editor coordinating the review of this manuscript and approving it for publication was Zhouyang Ren [ID].

there are two optional solutions which are mostly employed by the operators. The first solution is associated to increasing the current infrastructure of power system through adding the new substations and lines. The second solution is regarding to profiteering of the existent transmission and distribution system without upgrading, through optimal setting of the system parameters which results in improving the effectiveness of the system. This can be accomplished by carrying out technical study of power system that is called optimal power flow (OPF). OPF is utilized in an interconnected power system to obtain the optimized operating parameters of the system in such a way to achieve the predictable load dispatch with minimizing the total operating cost and real power losses [2]–[6]. Furthermore, OPF is divided to two sub problems, the first one is called economic dispatch problem and the second sub-problem is recognized as ORPD. The two

problems are implemented in different scenarios according to the requirement of objective functions [7], [8].

ORPD planning is mandatory requirement for viable and efficient operation of the power transmission and distribution systems. The solving ORPD problem has got attention through researchers in power system planning and operations [9], [10]. Solving the ORPD plays an important role in the system security, reliability, and economic operations. This is because it supports the voltage of the network to maintain it within desirable acceptable limits based on the proper coordination of the equipment that adjusts the flow of reactive power.

The objective of solving ORPD is minimizing a considered objective function, such as real power transmission losses, voltage deviation, and voltage stability index. These operational problems arise due to the complexity emerging in grid modernization. ORPD is fundamental to assist maintain the voltage level at the different loading state through reducing the voltage deviation as well as power quality issues which arise from the fluctuations of electrical power [11].

The considered objective function is achieved by adjusting the system control variables within different operating constraints. From a mathematical model optimization point of view, the problem of ORPD is a complex nonlinear problem, due to its nonlinear objective function and various type of constraints [12].

However, numerous efforts have been conducted for solving ORPD based on various classical optimization methods including linear and non-linear programming [13], [14], interior point method [15], [16] and decomposition algorithm [17], Regardless of the convergence characteristics of the classical optimization methods, these techniques may almost fail for obtaining the global solution due to difficulties of nonlinearity, and nonconvexity.

The metaheuristic optimization algorithms are inspired based on animals' behavior and physical phenomena have become widespread popular due to their flexibility, simplicity, ability to get global solutions, and prevent local optimal solutions [18]. The essence of metaheuristic techniques is based on the iterative correction solutions concept through generating new populations with implementing stochastic search operators [19]. Over recent years, there are growing attention on population-based and metaheuristics techniques for solving different power system optimization problems. These modern techniques have been extensively employed to overcome the problems of the conventional gradient-based optimization techniques [20], [21].

ORPD problem has been solved based on several metaheuristic optimization algorithms such differential evolution (DE) [22], [23], differential search algorithm [24], gravitational search algorithm (GSA) [25], enhanced marked algorithm [10], gray wolf optimizer [26], krill herd algorithm (KHA) [27], cuckoo search (CS) algorithm [28], ant-lion optimizer (ALO) [29], PSO with bat algorithm (BA) [30], Sine-Cosine algorithm (SCA) [31] and fractional order particle swarm optimization (FOPSO) [32].

Hybrid methods of more than one or two optimization algorithms can extract a synergy of their advantages simultaneously. This approach has been applied to develop several effective algorithms such as differential evolution algorithm (DDEA) and modified teaching learning-based algorithm (MTLBA) has been proposed in [33], hybrid firefly algorithm (FFA) and Nelder-Mead simplex method [34], modified imperialist competitive and invasive weed optimization (MICAIWO) [35], hybrid particle swarm optimization and Imperialist competitive algorithm (PSOICA) [36], hybrid chaotic (ABCDE) algorithm [37], hybrid PSO and GSA algorithm (PSOGSA) [9], hybrid PSO with artificial physics optimization (APO) (APOPSO) [38], and hybrid PSO and multi verse optimizer algorithm (PSOMVO) [11].

It worth noting that, these techniques may stuck in local optimal solution while solving complex multi-objective problems. Also, the convergence speed depends on the proper adjustment of the parameters of each metaheuristic [39], [40].

To improve the performance and effectiveness of metaheuristics techniques, various modifications maybe applied to them. Until now, chaos theory has been implemented on a broad of numerous metaheuristics and a wide range of applications for improving their performance to get better convergence and avoid getting stuck in a local minimum [41]. For example, of meta-heuristics that utilize chaos theory, the GSA technique [42], GWO technique [43], butterfly optimization algorithm (BOA) [44], salp swarm algorithm (SSA) [45], moth-flame optimizer (MFO) [46]. The metaheuristics based on chaos theory for solving the ORPD problem of different objective functions have been introduced in [47], [48] and Chaotic Bat Algorithm (CBA) with two modified techniques CBA_III and CBA_IV [49]. On the other hand, solving multi-objective ORPD problems based on different objective functions have been presented in the literature in [50] based on Pareto evolutionary algorithm for minimizing both active power loss and total voltage deviation. In [51], an improve voltage stability has been included in multi-objective ORPD problem with considering minimizing active power loss after that the problem has been solved using chaotic PSO. The modeling of ORPD as fuzzy goal programming for power loss reduction, improving voltage profile and enhancing static voltage stability then solved by genetic algorithm (GA) has been proposed in [52].

These metaheuristic techniques have their own demerits and merits in solving the ORPD problem, though definite complications are continued due to multi modal, discrete and nonlinear characteristic of power system that necessarily to be achieved in more adequate manners. Moreover, a wider set of utilized optimization techniques coverages towards sub optimal problem solutions due to the complex non-linear nature of the ORPD problems.

Therefore, solving ORPD problem is still a very important hot research issue in the electrical engineering due to its complexity, nonlinear characteristic of the system, and the stricter requirements of power quality. Hence, it is important

to develop new optimization methods that are capable of overcoming these barriers and handle the ORPD difficulties.

In this paper, an Improved Heap-based optimizer (IHBO) is proposed to solve ORPD for minimizing the most objective functions of the real power loss and total voltage deviation simultaneously based on the Pareto front technique. The original HBO is improved using the chaos theory. A circle chaotic map is employed to update the probability variable instead of using the random update function. The main contributions of this paper could be summarized in the following points:

- Proposing an improved version of the original HBO, called IHBO, with the aim of improving its performance and avoid getting stuck in a local optimum.
- Developing solution algorithms based on the original HBO and proposed IHBO to solve ORPD problem.
- Solving the bi and tri multi-objective solve ORPD problem based on the proposed IHBO and Pareto Optimal Front.
- Several objective functions such as minimizing the real power loss, total voltage deviations, and voltage stability index, are studied as single and multi-objective functions.
- Validating the proposed IHBO using several standard small and large test systems (IEEE 30-bus, IEEE 57-bus, and IEEE 118-bus).
- The simulation results confirm that IHBO has better performance or comparable superiority over other algorithms utilized in the literature.

The paper is presented as follows: Section II introduces the mathematical model of the ORPD problem. The IHBO algorithm is presented in Section III. In Section IV, the IHBO algorithm is implemented for solving the ORPD problem. The obtained results are introduced and discussed in section V. Finally, the conclusion is presented in Section VI.

II. THE MATHEMATICAL FORMULA OF ORPD

It is worth noting that, the ORPD problem is characterized as a complicated nonlinear optimization problem, however, it treated as a sub problem of optimal flow problem which determines the optimal output power of generators with the aim of minimizing a specific objective function considering several equality and inequality operating constraints. The objective functions in the present work are minimizing real power loss, the voltage deviations, and voltage stability index individually or simultaneously. The generator voltages, transformer tap settings, and reactive power of shunt capacitors are considered the control variables of the ORPD problem while the dependent variables are the load voltages, the flow of the lines, and the slack bus power.

A. OBJECTIVE FUNCTIONS

Mathematically, the formulation problem of the ORPD is expressed as follows [53], [35]:

$$minimize\ U\ (x, v) \tag{1}$$

Subject to constraints

$$z\ (x, v) = 0 \tag{2}$$

$$h\ (x, v) \leq 0 \tag{3}$$

where U is the objective function should be minimized, x is the vector consists of the control variables which represent the voltages of generators V_G, reactive power of shunt capacitors Q_{sc} and transformer tap settings T_S. However, x may be expressed as follows:

$$x^T = \begin{bmatrix} V_{G1}..., V_{GN_G}, Q_{SC}..., Q_{SCN_C}, T_{S1}..., T_{SN_T} \end{bmatrix} \tag{4}$$

where N_G, N_C and N_T define the number of generators, shunt Var compensators, and regulating transformers, respectively. v is the state vector consisting of the dependent variables which include the voltages at load buses V_L, the generated reactive power Q_G, the loading of the transmission line S_L and the power at slack bus P_{Gsl}. The state vector v is expressed as follows:

$$v^T = \begin{bmatrix} V_{L1}..., V_{LN_L}, Q_G..., Q_{GN_G}, S_{L1}..., S_{Ln_l}, P_{Gsl} \end{bmatrix} \tag{5}$$

where, N_L, and n_l depict the total number of load buses and transmission lines, respectively. Further, $z\ (x, v) = 0$ and $h\ (x, v) \leq 0$ represent the equality and inequality constraints, respectively.

1) MINIMIZATION OF TOTAL REAL POWER LOSS

The most objective function U considered in ORPD is that the total real power loss of the system. The ORPD solution aims to minimize the total real system loss in the transmission network. However, the minimization of real power loss acts as an important target for system operators, which can be formulated as follows [54]:

$$U_1\ (x_1, v_1) = min(P_L) = \sum_{k=1}^{n_l} G_k[V_i^2 + V_j^2 \\ - 2V_iV_jcos(\theta_i - \theta_j)] \tag{6}$$

where, P_L is the total real power loss, G_k is the conductance of k'th branch, V_i, V_j, θ_i and θ_j are the magnitudes and angles of voltage at bus i and j, respectively.

2) MINIMIZATION OF (TVD) AT LOAD BUSES

One of the most important indices for achieving the security of the system is minimizing the voltage deviations at load buses, to prevent the appearance of an unaccepted voltage profile. The voltage deviation is defined as the difference between the nominal reference voltage and the actual voltage. The voltage deviations are mathematically expressed as follows:

$$U_2\ (x_2, v_2) = min(TVD) = \sum_{k=1}^{N_L} |V_k - V_K^{Ref}| \tag{7}$$

where, TVD is the total voltage deviation, k is the element of the total number of load buses, V_k is the voltage magnitude at bus k, and V_K^{Ref} is the reference of the voltage magnitude at k th load bus and its value set to 1 p.u.

3) ENHANCEMENT OF VOLTAGE STABILITY

It's worth noting that, when the system subject to different operating situations such as disturbance or sudden load change, all buses should maintain acceptable bus voltage. L-index is the voltage stability index that plays an important role in voltage stability analysis. The values of the L− index is ranged from 0 to 1, where the lowest value refers to more stable system and vice versa [10]. The L-index of k'th bus is formulated as follows:

$$U_3(x_3, v_3) = min[max(L_k)] \quad k = 1, 2, 3..., N_L \quad (8)$$

where,

$$L_k = \left| 1 - \sum_{i=1}^{N_G} F_{ik} \frac{V_i}{V_k} \right| \quad (9)$$

$$F_{ik} = -[Y_A]^{-1}[Y_B] \quad (10)$$

where, i and k define the buses of generators and load, respectively. Y_A and Y_B depict the system sub-matrices for Y bus which obtained from the separation of generator and load buses.

B. THE PROBLEM CONSTRAINTS

The ORPD subject to equality and inequality operational constraints of the system as presented follows:

1) EQUALITY CONSTRAINTS

The following power balance equations are considered the equality constraints of the studied optimization problem.

$$P_{Gi} - P_{Di} - V_i \sum_{j=1}^{N_L} V_j(G_{ij}\cos\theta_{ij} + B_{ij}\sin\theta_{ij}) = 0 \quad (11)$$

$$Q_{Gi} - Q_{Di} - V_i \sum_{j=1}^{N_L} V_j(G_{ij}\sin\theta_{ij} - B_{ij}\cos\theta_{ij}) = 0 \quad (12)$$

where, P_{Gi} and Q_{Gi} are the output of active and reactive powers from the generator of bus i, respectively. P_{Di} and Q_{Di} are demand active and reactive powers of bus i, respectively. G_{ij} and B_{ij} are the branch conductance and susceptance between two buses, respectively.

2) INEQUALITY CONSTRAINTS

From (3), h represents the inequality constraints that including:

a: GENERATOR CONSTRAINTS

The voltages and reactive power outputs at all generating buses must be bounded within their upper and lower limits:

$$V_{Gi}^{min} \leq V_{Gi} \leq V_{Gi}^{max}, \quad i = 1, 2, 3 \ldots, N_G \quad (13)$$

$$Q_{Gi}^{min} \leq Q_{Gi} \leq Q_{Gi}^{max}, \quad i = 1, 2, 3 \ldots, N_G \quad (14)$$

$$P_{Gsl}^{min} \leq P_{Gsl} \leq P_{Gsl}^{max}, \quad i = 1, 2, 3..., N_C \quad (15)$$

where, $V_{Gi}^{min}, V_{Gi}^{max}$ are the minimum and maximum generating voltages of bus generating i'th, $Q_{Gi}^{min}, Q_{Gi}^{max}$ are the minimum and maximum generating reactive power of bus generator i'th and P_{Gsl}^{min}, P_{Gsl}^{max} are the minimum and maximum active power output of slack bus i'th.

b: CONSTRAINTS OF SHUNT VAR CAPACITORS

The upper and lower limits of the shunt reactive power compensators are represented as:

$$Q_{SCi}^{min} \leq Q_{SCi} \leq Q_{SCi}^{max}, \quad i = 1, 2, 3..., N_C \quad (16)$$

where, $Q_{SCi}^{min}, Q_{SCi}^{max}$ are the minimum and maximum shunt reactive power limits injected by the compensator i'th.

c: CONSTRAINTS OF TRANSMISSION LINE LOADING AND VOLTAGES AT LOAD BUSES

The inequality constraints of transmission line loading and voltages at load buses are represented as:

$$S_{li} \leq S_{li}^{max}, \quad i = 1, 2, 3..., n_l \quad (17)$$

$$V_{Li}^{min} \leq V_{Li} \leq V_{Li}^{max}, \quad i = 1, 2, 3..., N_L \quad (18)$$

where, S_{li}^{max} is the apparent power of the branch i'th, S_{li}^{max} indicates the maximum apparent power limit of branch i'th and V_{Li}^{min}, V_{Li}^{max} are the minimum and maximum load voltage magnitudes of i'th bus.

d: TRANSFORMER CONSTRAINTS

The constraints of transformers in the system are represented as:

$$T_i^{min} \leq T_i \leq T_i^{max} \quad i = 1, 2, 3..., N_T \quad (19)$$

where, T_i^{min}, T_i^{max} are the minimum and maximum tap transformer setting limits of i'th transformer.

The objective function including the inequality constraints is given as:

$$U_p = U_i + \lambda_v \sum_{k=1}^{N_L} \left(V_{Lk} - V_{Lk}^{lim} \right)^2 + \lambda_s \sum_{k=1}^{n_l} (S_{lk} - S_{lk}^{lim})^2$$
$$+ \lambda_q \sum_{k=1}^{N_G} (Q_{Gk} - Q_{Gk}^{lim})^2 \quad (20)$$

where, λ_v, λ_s and λ_q are the penalty factors. Further, the limit values of any variable in (20) are given as follows:

$$Y^{lim} = \begin{cases} Y_{max} & Y > Y^{max} \\ Y_{min} & Y < Y^{min} \end{cases} \quad (21)$$

where, Y^{lim} define V_L^{lim}, S_l^{lim} and S_l^{lim}.

III. ORIGINAL HBO

HBO is a human behavior based meta-heuristic that has been developed in [55]. It is based on the corporate rank hierarchy (CRH) in a very distinctive style. HBO's mathematical model is based on three pillars: (1) the relationship between subordinates and their immediate supervisor; (2) the relationship between colleagues; and (3) the employees' self-contribution. Heap data structure has been used in this manner to simulate the CRH. The using of the heap data structure in the CRH mapping allows organizing the solutions based

on their fitness in a hierarchy and using the arrangement in the algorithm's position-updating process in a very specific way. In this article, the mapping of the whole concept is divided into four steps: (i) modeling CRH, (ii) modeling the relationship between the subordinates and the immediate supervisor, (iii) modeling the interaction among colleagues, and (iv) an employee's self-contribution to executing a task.

A. IMPLEMENTATION OF THE CRH

Heap data structure has been used to implement the CRH where the heap is a data structure shaped by a non-linear tree. Hence, the entire CRH is considered as the population. In the implementation process, a search agent corresponds to a heap node. The search agent's fitness is the key to the heap node, and the population index of the search agent is the value of the heap node.

B. IMPLEMENTATION OF THE INTERACTION WITH THE IMMEDIATE BOSS

In a centralized organizational structure, laws and regulations are applied from the upper levels and subordinates obey their immediate supervisor. This can be mathematically modeled by updating the search agent's position as follows:

$$x_i^k(t+1) = B^k + \left| 2 - \frac{\left(t \bmod \frac{T}{C}\right)}{\frac{T}{4C}} \right| (2r-1) \left| B^k - x_i^k(t) \right| \quad (22)$$

where, x is the position of the search agent, B is the parent node, t and k are the current iteration and the number of the component vector, respectively, r is a random number between [0,1], T is the total number of iterations, and C is a defined parameter which has been set to $\frac{T}{25}$ based on the experimental study.

C. IMPLEMENTATION OF THE INTERACTION BETWEEN COLLEAGUES

Officials of the same rank are colleagues. To achieve official duties, they communicate with each other. In heap, it is assumed that the nodes are colleagues at the same level, and each search agent x_i updates its location according to the following equation about its randomly selected colleague S_r:

$$
\begin{aligned}
&x_i^k(t+1) \\
&= \begin{cases} S_r^k + \gamma \lambda^k \left| S_r^k - x_i^k(t) \right|, & f(S_r) < f(x_i(t)) \\ x_i^k + \gamma \lambda^k \left| S_r^k - x_i^k(t) \right|, & f(S_r) \geq f(x_i(t)) \end{cases}
\end{aligned} \quad (23)
$$

D. IMPLEMENTATION OF THE SELF-CONTRIBUTION OF AN EMPLOYEE

This implementation is very simple, where the position of the employee is retaining the previous position in the next iteration as follows:

$$x_i^k(t+1) = x_i^k(t) \quad (24)$$

E. OVERALL POSITION UPDATES

Based on the previous implementation, the position can be updated using different equations. However, these equations can be merged into one equation using probabilities parameters to balance exploration and exploitation phases. A roulette wheel is utilized to balance between these probabilities $p_1, p_2,$ *and* p_3.

Where, p_1 can be calculated as:

$$p_1 = 1 - \frac{t}{T} \quad (25)$$

and p_2 is expressed as:

$$p_2 = p_1 + \frac{1 - p_1}{2} \quad (26)$$

Finally, p_3 is calculated as:

$$p_3 = p_1 + \frac{1 - p_1}{2} \quad (27)$$

Hence, the overall position update equation can be written as follows:

$$x_i^k(t+1) = \begin{cases} x_i^k(t), \\ \qquad p \leq p_1 \\ B^k + \gamma \lambda^k \left| B^k - x_i^k(t) \right|, \\ \qquad p > p_1 \text{ and } p \leq p_2 \\ S_r^k + \gamma \lambda^k \left| S_r^k - x_i^k(t) \right|, \\ \qquad p > p_2 \text{ and } p \leq p_3 \text{ and } f(S_r) < f(x_i(t)) \\ x_i^k + \gamma \lambda^k \left| S_r^k - x_i^k(t) \right|, \\ \qquad p > p_2 \text{ and } p \leq p_3 \text{ and } f(S_r) \geq f(x_i(t)) \end{cases} \quad (28)$$

where, p is a random number within [0,1].

F. OVERALL HBO IMPLEMENTATION

The overall steps of HBO are presented in this section. Firstly, randomly initialize the population-based on control variables number N and the number of populations n as follows:

$$X = \begin{bmatrix} x_1^1 & \cdots & x_1^N \\ \vdots & \ddots & \vdots \\ x_n^1 & \cdots & x_n^N \end{bmatrix} \quad (29)$$

where, the population X must be within the boundary limits as:

$$X_{lb} \leq X \leq X_{ub} \quad (30)$$

Secondly, the heap is created using a d-array tree. In HBO, 3-arries is used to implement the CRH based on the following mathematical expression:

$$parent(i) = \left\lfloor \frac{i+1}{d} \right\rfloor \quad (31)$$

Eq. (33) is used to give the index of the parent node i in the heap array. A node can have up to 3 children in a 3-array heap. Hence, in the CRH mapping, it has been assumed that a supervisor cannot have more than 3 direct subordinates. Therefore, the mathematical formulation of the child j for node i can be written as:

$$child(i, j) = d \times i - d + j + 1 \quad (32)$$

In a 3-array heap, the depth of any node i can be calculated as:

$$depth(i) = \lceil log_d(d \times i - i + 1) \rceil - 1 \quad (33)$$

To describe the colleague which are all nodes at the same level of a node i, a colleague (i) is used to generate a random integer in the range as follows:

$$colleague(i) = \left[\frac{d \times d^{depth(i)-1}}{d-1} + 1, \frac{d \times d^{depth(i)}}{d-1} \right] \quad (34)$$

Heapify_Up (i): it searches upward in the heap and inserts the node i at its correct location to maintain the heap property. Then, a heap is built for the population where heap_value is used to store the indices of the search agents into the population and heap_key is used to stores the fitness of the corresponding search agents. Thirdly, search agents repeatedly update their positions following previously discussed equations and try to converge on the global optimum. The flowchart of the HBO is shown in Fig.1.

IV. PROPOSED HBO

Chaos maps have been used in many fields for forecasting erratic behaviors such as atmosphere, brain conditions, or turbulent movement of air or water. Recently, in optimization algorithms, several chaotic maps have been used. The key benefit of using chaotic maps in optimization is to increase the algorithm's convergence rate using various chaotic maps as an alternative for using random variables. To improve the performance of the original HBO, a chaotic map is involved to change the probability variable p instead of using the random function as follows:

$$p_{k+1} = mod\left(p_k + b_1 - \left(\frac{b_2}{2\pi}\right) sin(2\pi p_k), 1\right)$$
$$\times b_1 = 0.5, \quad b_2 = 0.2 \quad (35)$$

A. MULTI-OBJECTIVE HBO

The single objective IHBO is considered the main core of the multi-objective IHBO (MOIHBO). In the multi-objective algorithms, Pareto dominance is employed to compromise among the objective functions. Therefore, the solutions obtained are categorized as dominated and non-dominated solutions. Then, the optimal solution will be chosen from the non-dominated alternatives by the decision-maker. In this regard, two functions are used to formulate the Pareto optimal solutions from the IHBO, namely archive and leader selection. The archive is responsible for organizing the non-dominant solutions accomplished so far and the selection of leaders used to direct the other agents to obtain the right solution. The MOIHBO is shown in Algorithm 1.

B. COMPROMISE SOLUTION

A fuzzy membership approach is applied to achieve the best compromise solution. A membership function u_i^n is represented for the all n functions at each i non-dominated solution
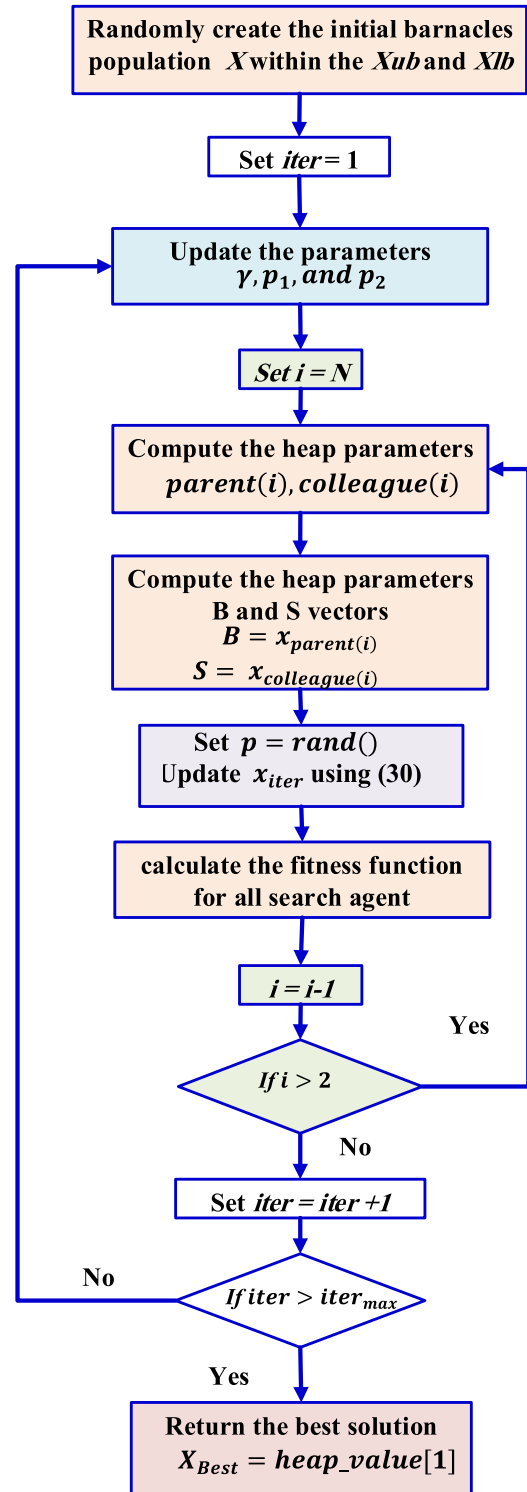

FIGURE 1. HBO implementation flowchart.

as follows:

$$u_i^n = \begin{cases} 1 & F_i \leq F_i^{min} \\ \frac{F_i^{max} - F_i}{F_i^{max} - F_i^{min}} & F_i^{max} \leq F_i \leq F_i^{min} \\ 0 & F_i \geq F_i^{max} \end{cases} \quad (36)$$
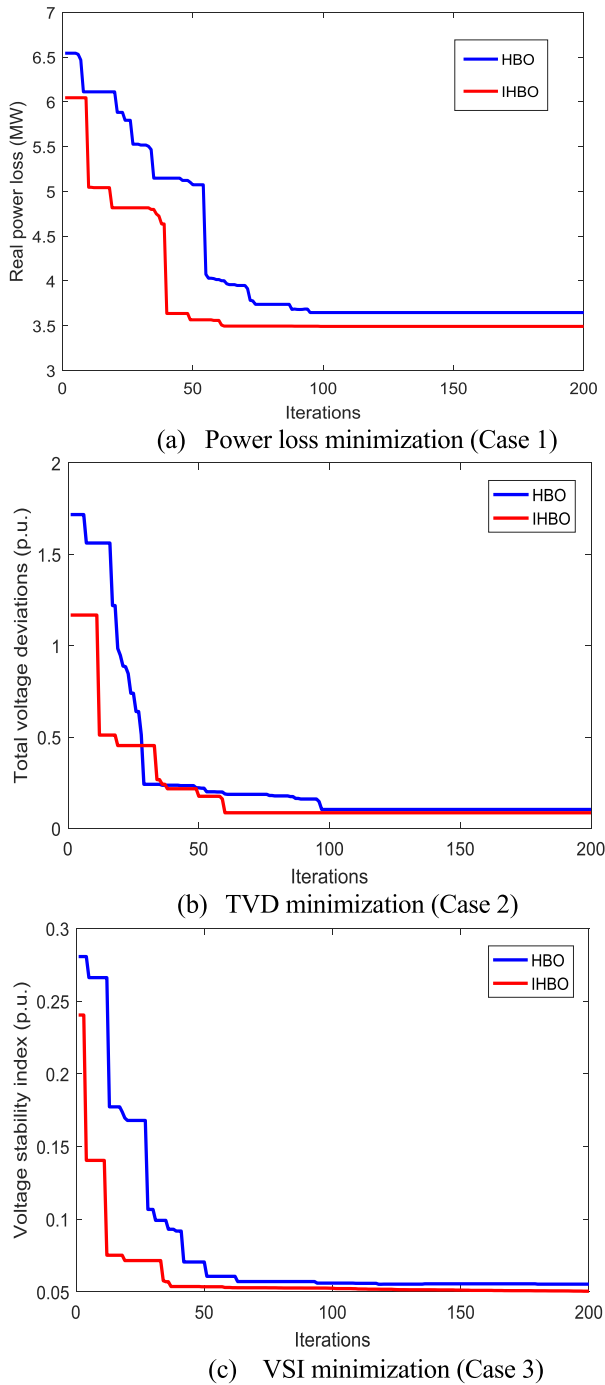
(a) Power loss minimization (Case 1)

(b) TVD minimization (Case 2)

(c) VSI minimization (Case 3)

FIGURE 2. Convergence characteristics of HBO and IHBO for single objective function (IEEE 30-bus system).

where, F_i^{min} and F_i^{max} are the minimum and maximum value of the ith objective function among all non-dominated solutions, respectively. Hence, the normalized value for each non-dominated solution is calculated as follows:

$$u^n = \frac{\sum_{i=1}^{nobj} u_i^n}{\sum_{n=1}^{M} \sum_{i=1}^{nobj} u_i^n} \qquad (37)$$

where, M denotes the total number of the non-dominated solution, therefore, the best compromise solution is the one with the highest value of u^n.

Algorithm 1 MOIHBO Formulation

1: **Initialize** a set of random search agents x_i^k
2: **Calculate** the objective functions for each search agent
3: **Find** the non-dominate solutions and store in the archive
4: **Select** the leader using leader selection
5: **while** ($iter < iter_{max}$)
6:     **for** each search agents x_i^k
7:         **Update** the position using (30)
8:         **Calculate** the objective functions
9:         **Find** the non-dominate solutions and update the archive
10:        **if** the archive is full
11:            **Run** the grid mechanism to omit one of the current archive members
12:            **Add** the new solution to the archive
13:        **endif**
14:        **if** any of the new added solutions to the archive is located outside the hypercubes
15:            **Update** the grids to cover the new solution(s)
16:        **endif**
17:        **Perform** the leader selection
18:        $iter = iter + 1$
19: **end while**
20: **return** final non-dominated solutions stored in the archive

---
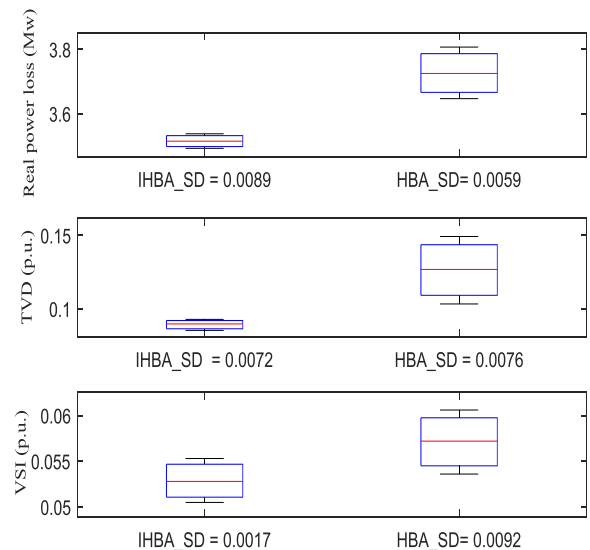
FIGURE 3. The statistical results for all single objective functions of ORPD (IEEE 30-bus system).

V. SIMULATION RESULTS AND DISCUSSION

To prove the effectiveness and performance of the proposed IHBO, both original HBO and IHBO are used to solve the standard test systems; IEEE 30-bus, IEEE 57-bus and IEEE 118-bus with the aim of minimizing the real power loss, total voltage deviations, and voltage stability index as single objective and multi-objective functions. All simulation studies have been run on MATLAB 2016a, 2.8 GHz Intel Pentium

TABLE 1. The optimal variables obtained by HBO and IHBO based on the single objective ORPD problem (IEEE 30-bus system).

Optimal Variables	IHBO			HBO		
	Minimization of real losses Case1	Minimization of TVD Case2	Minimization of VSI Case3	Minimization of losses Case1	Minimization of TVD Case2	Minimization of VSI Case3
VG1(p.u.)	1.0852	1.0209	1.0918	1.0730	1.0297	1.1000
VG2 (p.u.)	1.0785	1.0224	1.0850	1.0656	1.0285	1.0823
VG5 (p.u.)	1.0583	1.0190	1.0676	1.0468	1.0204	1.0492
VG8 (p.u.)	1.0619	0.9970	1.0700	1.0491	1.0004	1.0258
VG11 (p.u.)	1.0927	1.0730	1.0631	1.1000	0.9926	1.0122
VG13 (p.u.)	1.0999	0.9966	1.0983	1.0999	0.9885	1.0515
T11(p.u.)	0.9707	0.9964	1.0522	0.9739	0.9942	1.0024
T12(p.u.)	0.9571	0.9810	0.9087	0.9046	0.9243	0.9836
T15(p.u.)	0.9808	0.9547	0.9655	0.9585	0.9446	0.9922
T36(p.u.)	0.9616	0.9578	0.9400	0.9373	0.9686	0.9000
QC10(MVAR)	4.4825	3.3119	1.4608	4.9982	5.0000	1.8658
QC12(MVAR)	4.5535	2.0072	2.9488	5.0000	2.4770	5.0000
QC15(MVAR)	3.3129	4.2176	2.7769	4.6281	4.9742	2.0750
QC17(MVAR)	4.7386	0.0578	1.7870	4.9974	3.2193	0.4524
QC20(MVAR)	4.8276	4.1348	4.6215	4.9032	4.9976	1.6272
QC21(MVAR)	4.8112	2.7192	1.2657	5.0000	4.9677	0.5962
QC23(MVAR)	4.2528	4.9480	4.1981	4.1526	4.5193	1.5398
QC24(MVAR)	4.9770	4.9673	3.3160	4.9920	4.9963	4.3167
QC29(MVAR)	2.7511	2.0293	2.3654	2.9582	3.8763	3.4728
loss (MW)	3.4923	4.2417	3.6435	3.6469	4.3519	4.7557
TVD (p.u.)	1.4794	0.0854	1.0658	1.9244	0.1034	0.9118
VSI(p.u.)	0.1251	0.2106	0.0505	0.1576	0.1846	0.0536
Time(s)	86.8394	65.0814	70.4705	95.9941	71.9525	77.2185

i7 PC with 16 GB of RAM. The numerical optimal values have been obtained for the two algorithms after 200 iterations for all test systems. Moreover, the simulation studies have been obtained after 30 independent runs for all the test cases. The two algorithms have been implemented on a total population of 50 particles.

A. IEEE 30-BUS TEST SYSTEM

The IEEE 30-bus test system consists of 6 generators with one slack bus, 41 branches (transmission lines of 37 branches and tap changing transformers of 4 branches), 9 reactive power compensators and the total real and reactive power demand of the system are 238.4 MW and 126.2 MVAR, respectively. The detailed data of buses and lines for the IEEE 30-bus system are defined in [54]. Further, in this study, the system level is constrained as follows, the voltage magnitude range is 0.95 p.u. and 1.1 p.u. for all generating buses. The limits between 0.95 p.u. bus 1.05 p.u. are considered for load buses voltages. On the other hand, the tap changing transformers are ranged from 0.9 p.u. to 1.1 p.u. In addition, the limits of shunt VAR compensators are supposed between 0 to 5 MVAR. This system comprises 19 control variables including 6 generators, 4 settings of tap changing transformers, and 9 shunt VAR capacitors.

1) SINGLE-OBJECTIVE ORPD FRAMEWORK

In this subsection, the effectiveness of the proposed IHBO to solve the ORPD problem as single objective function (minimization of the total real power loss or TVD or VSI) is proved. The results obtained by the proposed IHBO are compared with those obtained by the original HBO and other well-known optimization algorithms. The obtained results for all cases are listed in Table 1. The results that are reported at the base case of the test system are acquired from previous literature [56]. The three considered single objective functions are presented as follows:

Case 1: this case aims to minimize the total real power loss based on the original HBO and proposed IHBO. However, the real power loss is minimized to 3.6469 MW and 3.4923 MW using HBO and IHBO, respectively. By HBO, the TVD and VSI are minimized to 1.9244 p.u. and 0.1576, respectively, while they are minimized to 1.4794 p.u. and 0.1251, respectively by IHBO.

Case 2: the main objective function in this case, is to minimize the TVD using the two algorithms. The TVD is reduced to 0.1034 p.u and 0.0854 p.u. using HBO and IHBO, respectively. In contrast, the real power loss, and VSI became 4.3519 MW and 0.1846, respectively by HBO, while the

TABLE 2. Results of single-objective ORPD obtained using different optimization techniques (IEEE 30-bus system).

OF (s)	DE	GSA	SCA	MJAYA	CLPSO	PSOGSA	APOPSO	HBO	IHBO
Minimization of losses	4.555	4.5143	4.8139	4.6234	4.5615	4.5309	4.3980	3.6469	3.4923
Minimization of TVD	0.0911	0.0676	0.4183	0.1316	0.2450	0.0904	0.0870	0.1034	0.0854
Minimization of VSI	0.1246	0.1368	0.1255	0.0922	0.0866	0.0950	0.1227	0.0536	0.0505

TABLE 3. The optimal results obtained by IHBO based on multi-objective ORPD problem (IEEE 30-bus system).

Optimal variables	Case 4	Case 5	Case 6	Case 7
V G1(p.u.)	1.0498	1.0829	1.0432	1.0503
VG2 (p.u.)	1.0434	1.0773	1.0227	1.0417
VG5 (p.u.)	1.0278	1.0679	1.0016	1.0147
VG8 (p.u.)	1.0239	1.0687	1.0026	1.0236
VG11 (p.u.)	1.0947	1.0758	0.9849	1.0405
VG13 (p.u.)	1.0362	1.0833	1.0096	1.0462
T11(p.u.)	0.9789	1.0115	0.9942	0.9364
T12(p.u.)	1.0666	0.9000	0.9508	1.0625
T15(p.u.)	1.0254	1.0459	0.9514	0.9879
T36(p.u.)	0.9888	0.9961	0.9449	0.9758
QC10(MVAR)	0.0000	4.9008	0.0000	2.9206
QC12(MVAR)	4.2572	4.4311	5.0000	2.1540
QC15(MVAR)	1.8970	5.0000	5.0000	1.8964
QC17(MVAR)	0.3227	5.0000	5.0000	5.0000
QC20(MVAR)	2.6588	2.4524	5.0000	3.8982
QC21(MVAR)	1.2625	5.0000	5.0000	0.0658
QC23(MVAR)	2.4521	0.0000	0.2426	1.7519
QC24(MVAR)	3.8074	3.7001	5.0000	4.0005
QC29(MVAR)	2.9734	1.2890	3.3279	1.3976
loss (MW)	3.8842	3.6188	4.2338	3.9254
TVD (p.u.)	0.2955	0.9677	0.2163	0.3134
VSI(p.u.)	0.2249	0.0838	0.0583	0.0968

real power loss, and VSI became 4.2417 MW and 0.2106, respectively by IHBO.

Case 3: in this case, VSI is taken as the main objective function utilizing both HBO and IHBO. In this case, the VSI is minimized to 0.0536 by HBO and 0.0505 by IHBO. On the other hand, the real power loss and TVD are equal to 4.7557 MW and 0.9118 p.u, respectively by HBO, while, these values are equal to 3.6435 MW and 1.0658 p.u., respectively by IHBO.

Table 2 provides the best values of the three considered objective functions obtained by the original HBO, the proposed IHBO and the other well-known algorithms, PSO-GSA [12], (DE) [22], GSA [25], SCA [31], APOPSO [38], MJAYA [54], and comprehensive learning particle swarm optimization (CLPSO) [57]. From Table 2, it can be observed that the IHBO outperforms other techniques, where it

provides the lower values all three objective functions compared with other algorithms.

The convergence characteristics of real power loss, TVD, and VSI for 200 iterations yielded by both HBO and IHBO for IEEE 30-bus are shown in Fig. 2. It can be observed that the proposed IHBO reaches to the optimal solution faster than the original HBO.

Fig.3. shows the statistical results yielded by two algorithms based on the three considered single objective functions through 30 independent trials which conducted for each algorithm to compare their best, worst, mean values and standard deviation (SD).

2) MULTI-OBJECTIVE OF ORPD FRAMWORK
In this subsection, the optimal values of real power loss, TVD, and VSI are obtained by the developed multi-objective
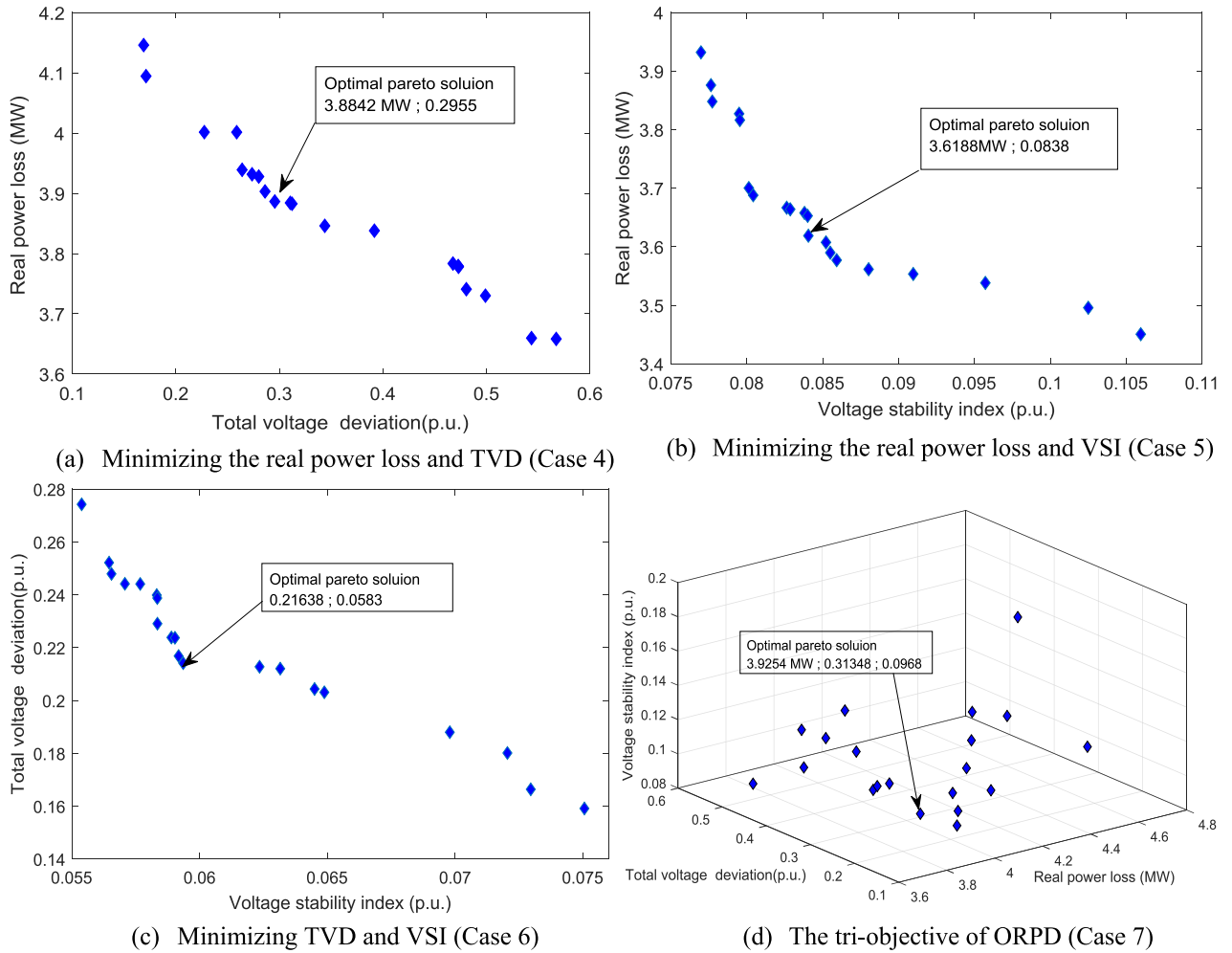
(a) Minimizing the real power loss and TVD (Case 4)

(b) Minimizing the real power loss and VSI (Case 5)

(c) Minimizing TVD and VSI (Case 6)

(d) The tri-objective of ORPD (Case 7)

FIGURE 4. Pareto set using IHBO based on multi-objective ORPD (IEEE 30-bus system).

HBO and IHBO algorithms. However, two models of multi-objective problems namely bi and tri objective functions are considered here. The simulation results based on multi-objective IHBO are tabulated in Table 3. Fig. 4 shows the generated Pareto optimal results for all cases of multi-objective functions of the IEEE 30 bus test system. The studied cases of multi-objective ORPD problems are described as:

Case 4: both HBO and IHBO are utilized for minimizing the real power loss and TVD simultaneously. The Pareto front values are shown in Fig.4a for this case. On the other hand, the optimal variables along with the best values of objective functions are listed in Table 3. From this table, it is seen that the ability of IHBO for obtaining the best values of real power loss and TVD which are 3.8842 MW and 0.2955 p.u., respectively.

Case 5: In this case, the real power loss, and VSI are considered as bi-multi-objective function. Pareto front obtained by IHBO is shown in Fig.4b. However, the optimal variables and the corresponding minimum values of the bi multi-objective problem are presented in Table 3. From this

table, it can be displayed that the best values for real power loss and VSI are 3.6188 MW and 0.0838 p.u., respectively.

Case 6: In this case, the TVD and VSI are optimized simultaneously. The Pareto front acquired by the proposed IHBO is shown in Fig.4c. In addition, the simulation results of optimal variables with the best values of each considered objective function are listed in Table 3. The preferable compromise values for TVD and VSI are 0.2163 and 0.0583, respectively.

Case 7: in this case, the results of the tri objective ORPD problem are presented. The real power loss, TVD, and VSI are optimized simultaneously. The Pareto front acquired using IHBO is displayed in Fig.4d. The best values of the three objective functions and the corresponding optimal control variables are tabulated in Table 3. From this table, it can be observed that the best values for the real power loss, TVD and VSI are 3.9254 MW, 0.31348, 0.0968 p.u., respectively.

B. IEEE 57-BUS TEST SYSTE

The IEEE 57-bus test system comprises 7 generating units with one slack bus, 80 transmission lines and 17 tap changing transformers, 3 reactive power compensators.

TABLE 4. The optimal values obtained by HBO and IHBO based on the single objective ORPD problem (IEEE 57-bus system).

Optimal Variables	IHBO			HBO		
	Minimization of real losses Case8	Minimization of TVD Case9	Minimization of VSI Case10	Minimization of losses Case8	Minimization of TVD Case9	Minimization of VSI Case10
V G1(p.u.)	1.0141	1.0439	1.0113	1.0879	1.0223	1.0667
VG2 (p.u.)	1.0066	1.0335	1.0023	1.0780	1.0037	1.0425
VG3(p.u.)	1.0044	1.0183	1.0014	1.0633	1.0134	1.0240
VG6 (p.u.)	1.0164	1.0034	1.0087	1.0432	1.0087	1.0075
VG8 (p.u.)	1.0073	0.9851	1.0084	1.0351	1.0234	1.0084
VG9 (p.u.)	0.9790	0.9762	0.9942	1.0071	0.9979	0.9975
VG12 (p.u.)	0.9880	0.9934	1.0155	0.9875	1.0049	1.0207
T19(p.u.)	1.0543	1.0836	1.0004	0.9842	0.9049	1.0071
T20 (p.u.)	0.9938	1.0737	0.9694	1.0325	1.0530	0.9800
T31 (p.u.)	0.9519	0.9613	1.0724	0.9810	0.9588	1.0314
T35 (p.u.)	1.0748	0.9244	1.0691	0.9124	0.9841	0.9694
T36 (p.u.)	1.1000	1.0046	0.9650	1.0321	1.0116	0.9683
T37 (p.u.)	1.0628	0.9860	1.0258	0.9638	1.0997	1.0576
T41(p.u.)	0.9899	0.9310	1.0396	0.9689	0.9534	0.9338
T46 (p.u.)	1.0385	1.0371	1.0040	1.0007	1.0735	1.0699
T54 (p.u.)	0.9000	0.9633	1.0051	1.0510	0.9650	1.0596
T58 (p.u.)	0.9657	0.9825	1.0005	0.9541	1.0092	1.0799
T59 (p.u.)	0.9000	0.9274	0.9105	1.0334	0.9004	0.9206
T65 (p.u.)	0.9000	0.9000	0.9590	0.9105	0.9065	0.9436
T66 (p.u.)	0.9109	0.9462	0.9323	0.9483	0.9654	0.9077
T71 (p.u.)	0.9346	0.9011	0.9614	1.0113	0.9448	0.9137
T73 (p.u.)	0.9889	1.0058	0.9240	0.9350	1.0997	1.0155
T76 (p.u.)	1.1000	1.0385	0.9922	0.9308	0.9303	1.0103
T78 (p.u.)	1.0107	1.0032	1.0175	0.9504	0.9398	0.9571
QC18(MVAR)	0.0000	13.6102	17.9494	22.0154	3.8022	8.1152
QC25(MVAR)	17.7207	16.2686	13.2188	18.5704	18.4981	15.4811
QC53(MVAR)	21.9258	23.3757	22.8630	9.1632	15.3399	21.3262
loss (MW)	13.9725	16.4291	19.4196	14.7935	18.7449	21.1385
TVD (p.u.)	1.1208	0.8781	1.2387	1.3781	1.0354	1.3069
VSI (p.u.)	0.8079	0.8626	0.5085	0.8835	0.8168	0.6291

TABLE 5. Results of single-objective ORPD obtained by different optimization techniques (IEEE 57-bus system).

OF (s)	SR-DE	ALC-PSO	MICA-IWO	SOA	CKHA	APOPSO	CBA_IV	CBA_III	BA	GSA	HBO	IHBO
Minimization of losses	23.3550	23.3900	24.2568	24.2654	23.4100	14.9920	21.9627	22.0162	22.0300	23.4600	14.7936	13.9725
Minimization of TVD	NA	0.6634	NA	NA	0.6600	0.9430	0.6399	0.6413	0.6434	1.1100	1.0354	0.8781
Minimization of VSI	NA	NA	NA	0.1907	0.1897	0.1134	0.1608	0.1789	0.1917	NA	0.6291	0.5085

The total real and reactive power load demands of the system are 1250.8 MW and 336.4 MVAR, respectively. The detailed data of this test system are given in [59].

Moreover, in this paper the system constraints are limited as follows, for all generating buses, the magnitudes of voltage are limited from 0.9 p.u. to 1.1 p.u. The voltage limits are taken between 0.94 p.u. bus 1.06 p.u. at load buses. The tap changing transformers are varied between 0.9 p.u. to 1.1 p.u. Limits of reactive power compensation devices are assumed between 0 to 30 MVAR. Overall, the IEEE 57-bus test system comprises 27 control variables comprehensive 7 generating units, 17 tap changing transformers, and 3 shunt VAR compensation devices.

1) SINGLE-OBJECTIVE ORPD

In this subsection, the proposed IHBO is also validated for solving the single-objective ORPD problem described in (20) of the IEEE 57-bus test system. The obtained optimal variables for the three considered Cases 8–10, are given in Table 4. These cases can be summarized as:

Case 8: This case aims to minimize the total real power loss using HBO and IHBO. The total real power losses are 14.7935 MW and 13.9725 MW using HBO and IHBO, respectively. Further, the TVD and VSI are equal to 1.3780 p.u. and 0.8835, respectively using HBO as well, the TVD and VSI are equal to 1.1208 p.u. and 0.8079, respectively using IHBO.
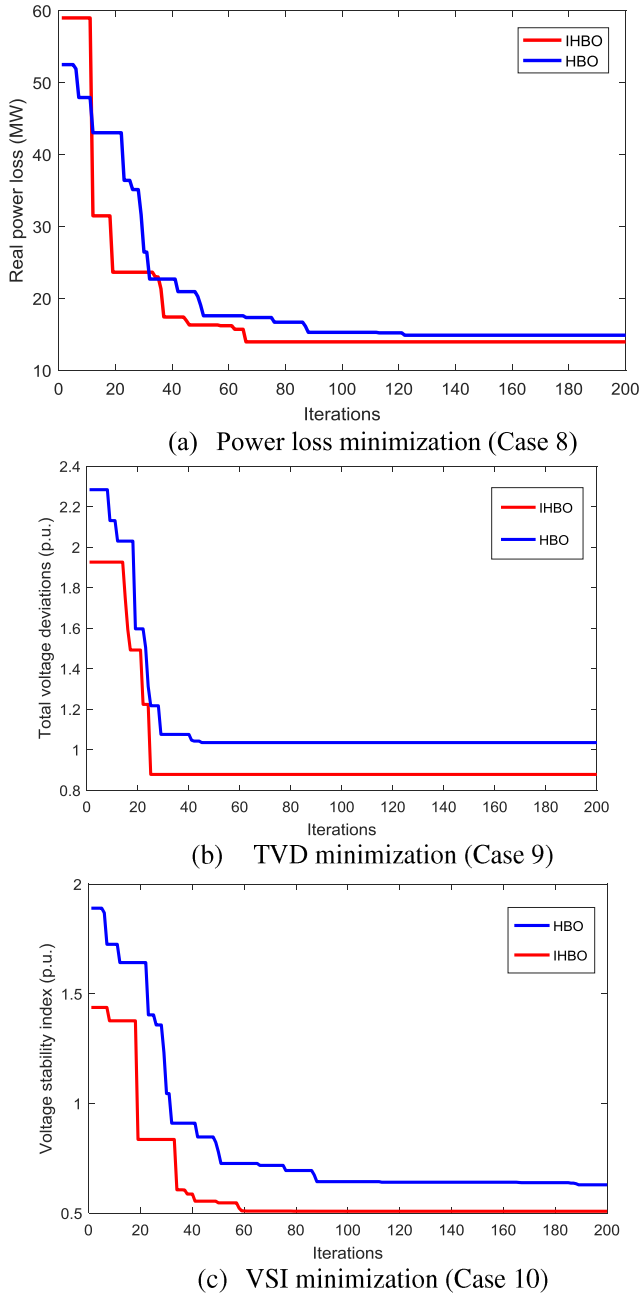
(a) Power loss minimization (Case 8)

(b) TVD minimization (Case 9)

(c) VSI minimization (Case 10)

FIGURE 5. Convergence characteristics of HBO and IHBO of HBO and IHBO for single objective function (IEEE 57-bus system).

FIGURE 6. The statistical results for all single objective functions of ORPD (IEEE 57-bus system).

1.3069 p.u., respectively. As well, these values using IHBO are equal to 19.4196 MW and 1.2387 p.u., respectively.

To confirm the superiority and effectiveness of the proposed IHBO, the objective function results using HBO and HBO are compared with those obtained by other recently reported algorithms. The best values of the studied single objective functions obtained by different optimization algorithms are tabulated in Table 5. The IHBO presents the best capabilities for minimizing the objective function compared with HBO, GSA [25], APOPSO [38], BA, CBA_III and CBA_IV [49], CKHA [58], Seeker optimization algorithm (SOA) [60], adaptive invasive weed optimization algorithm (MICA-IWO) [61], PSO with an aging leader and challengers (ALC-PSO) [62], and stochastic ranking with differential evolution SR-DE [63].

The convergence characteristics yielded by both HBO and IHBO for single-objective functions of the ORPD problem over IEEE 57-bus are shown in Fig.5. This figure displays the robust performance of the IHBO for larger extent systems.

The statistical results are obtained and compared using HBO and IHBO, which are utilized for solving single-objective ORPD through 30 independent trials performed for each algorithm and the results are presented in Fig 6.

2) MULTI-OBJECTIVE ORPD

As stated in the previous subsection of IEEE 30-bus test system, two models of multi-objective problems are utilized called bi and tri-objective functions. The simulation results obtained by the IHBO for the considered cases are presented in Table 6. Furthermore, Fig.7 depicts the produced Pareto optimal values for two considered models of multi-objective functions based on four cases implemented over the IEEE 57-bus test system, which are described as follows:

Case 9: the main objective function is to minimize the TVD using HBO and IHBO. As seen from the results, the TVD is 1.0354 p.u. and 0.8781 p.u. using HBO and IHBO, respectively. Moreover, the total real power loss and VSI are equal to 18.7449 MW and 0.8168, respectively using HBO. Likewise, the total real power loss and VSI are equal to 16.4291MW and 0.8626, respectively using IHBO.

Case 10: the main objective function in this case, is to minimize the VSI. Using HBO and IHBO, the VSI is minimized to 0.6291 and 0.5085, respectively. In contrast, the real power loss and TVD using HBO are equal to 21.1385 MW and
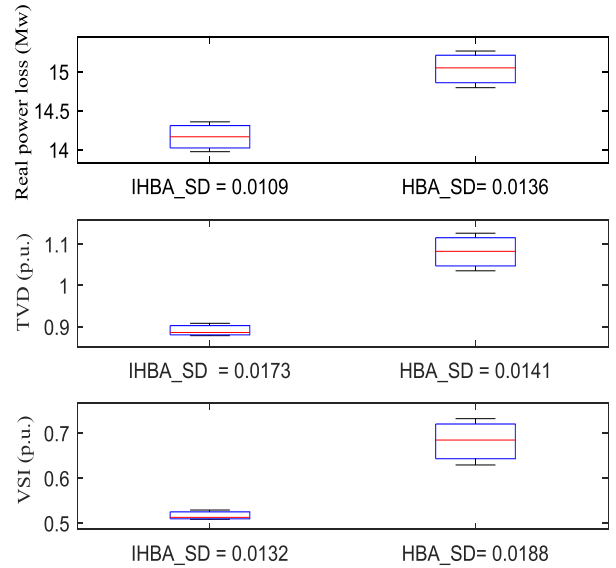
(a) Minimizing the real power loss and TVD (Case 11)

(b) Minimizing the real power loss and VSI (Case 12)

(c) Minimizing TVD and VSI (Case 13)
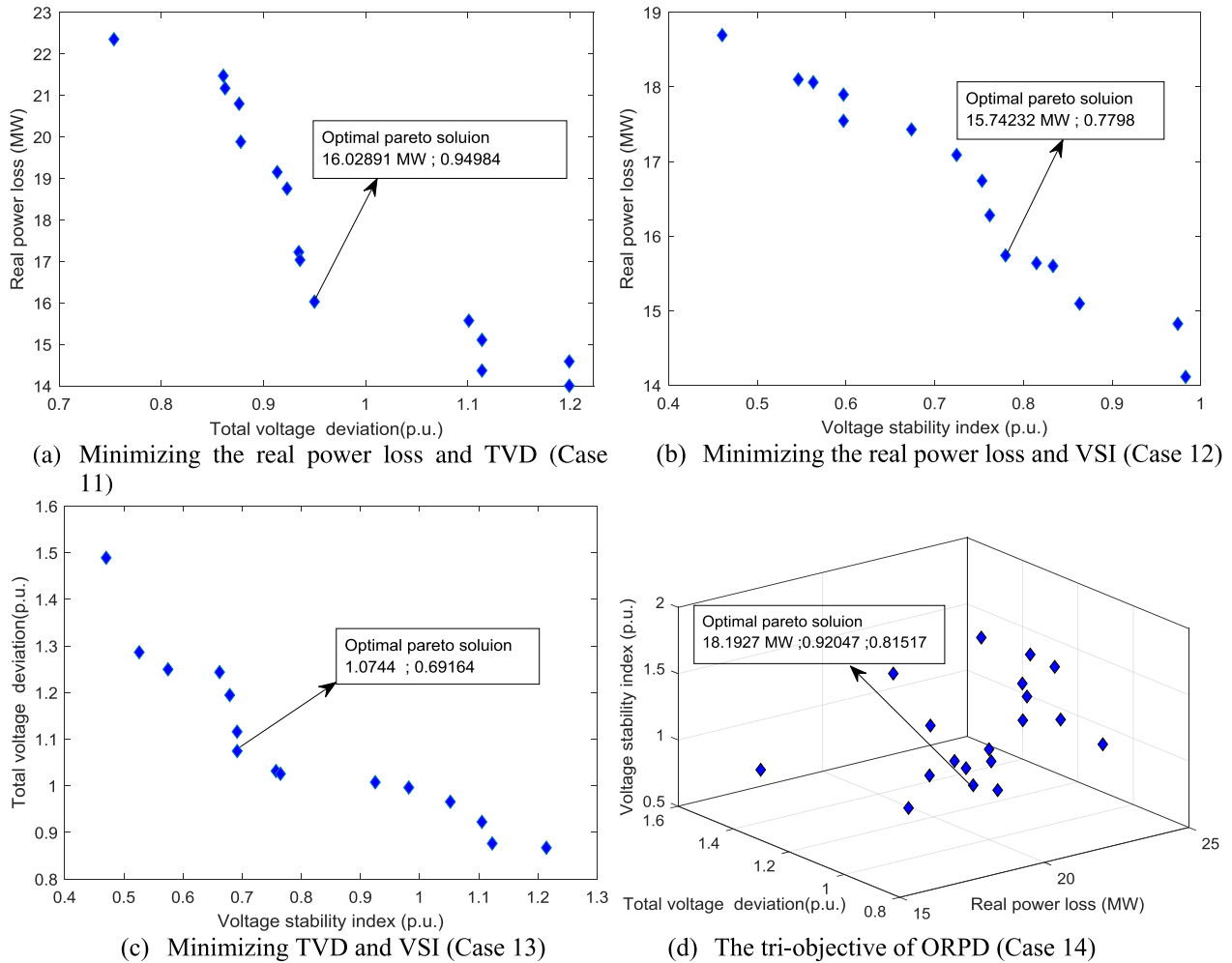
(d) The tri-objective of ORPD (Case 14)

FIGURE 7. Pareto set using IHBO based on multi-objective ORPD (IEEE 57-bus system).

Case 11: IHBO is applied in this case for minimizing the real power loss and TVD simultaneously. The values of the Pareto front are shown in Fig.7a. As well, the optimal variables and the best values of objective functions to be minimized in this case are given in Table 6. It is seen from the table, the capability of IHBO for achieving the best minimum values of real power loss and TVD which are equal to 16.0289 MW and 0.9498 p.u., respectively.

Case 12: The real power loss and VSI are solved as a bi multi-objective problem for minimizing each of them simultaneously. The Pareto front based on the proposed IHBO are shown in Fig.7b. The minimum values of the bi multi-objective problem and the optimal variables are introduced in Table 6. The results show that the best optimization values for real power loss and VSI are equal to 15.7423 MW and 0.7799 p.u., respectively.

Case 13: In this case, the TVD and VSI are minimized simultaneously using the proposed IHBO based on the bi multi-objective model. The Pareto front are displayed in Fig.7c. Moreover, the simulation results of optimal variables with the minimum values of the TVD and VSI are

presented in Table 6. The preferable results for TVD and VSI are 1.0745 p.u. and 0.6916, respectively.

Case 14: the tri multi-objective ORPD problem is solved using the proposed IHBO. The Pareto front of the three considered objective functions is displayed in Fig.7d. The best minimum values of three objective functions along with the optimal variables are listed in Table 6. The best values for the real power loss, TVD and VSI are 18.1928 MW, 0.9205 p.u. and 0.8152 respectively.

C. IEEE 118-BUS TEST SYSTEM

To achieve the robustness and strength performance 186 of IHBO based on the large-scale test system, the IHBO is applied in this section on the IEEE 118-bus test system. The system comprises 54 generating units, 64 load buses, transmission lines, 14 reactive power compensators, and 9 tap-setting transformers. Further, the total load of real and reactive power is 4242 MW and 1438 MVAR, respectively. The detailed system technical data are presented in [64].

Furthermore, the system constraints are as follows; the limits of voltage magnitudes at the generating buses are between

TABLE 6. The optimal values obtained by IHBO based on multi-objective ORPD problem (IEEE 57-bus system).

Optimal variables	Case 11	Case 12	Case 13	Case 14
V G1(p.u.)	1.1000	1.0329	1.0504	1.0749
VG2 (p.u.)	1.0835	1.0111	1.0279	1.0497
VG3(p.u.)	1.0662	1.0090	1.0305	1.0319
VG6 (p.u.)	1.0610	1.0038	1.0271	1.0037
VG8 (p.u.)	1.0567	0.9868	1.0300	0.9770
VG9 (p.u.)	1.0274	0.9752	1.0151	0.9878
VG12 (p.u.)	1.0151	0.9894	1.0400	1.0388
T19(p.u.)	0.9496	1.0356	0.9959	0.9061
T20 (p.u.)	0.9842	0.9477	1.0380	1.0752
T31 (p.u.)	0.9655	1.1000	0.9000	1.0415
T35 (p.u.)	0.9088	0.9059	1.0855	1.0307
T36 (p.u.)	1.0307	1.0102	0.9956	0.9855
T37 (p.u.)	1.0570	1.0413	1.0512	1.0454
T41(p.u.)	1.0106	0.9986	0.9906	1.0064
T46 (p.u.)	0.9889	1.0299	1.0712	1.0053
T54 (p.u.)	0.9034	0.9602	0.9001	0.9012
T58 (p.u.)	1.0526	0.9198	0.9557	0.9641
T59 (p.u.)	0.9514	0.9014	0.9476	0.9200
T65 (p.u.)	0.9995	0.9636	1.0154	1.0784
T66 (p.u.)	1.0663	0.9685	0.9878	0.9882
T71 (p.u.)	1.0555	1.0191	0.9444	0.9712
T73 (p.u.)	1.0237	0.9000	1.1000	0.9052
T76 (p.u.)	0.9140	1.0221	0.9923	1.0608
T78 (p.u.)	1.0241	0.9175	0.9703	0.9902
QC18(MVAR)	0.0421	15.3005	7.6568	24.6084
QC25(MVAR)	15.7695	19.0355	17.3871	12.2347
QC53(MVAR)	11.2935	30.0000	2.8277	29.9924
loss (MW)	16.0289	15.7423	21.6997	18.1928
TVD (p.u.)	0.9498	1.2133	1.0744	0.9204
VSI(p.u.)	0.8898	0.7798	0.6916	0.8152

0.9 p.u. and 1.1 p.u., the limits of voltages at load buses are considered between 0.94 p.u. bus 1.06 p.u., the tap-setting transformers are considered between 0.9 p.u. to 1.1 p.u., the limits of shunt reactive compensators are supposed to be between 0 to 20 MVAR.

The system comprises 77 control variables including 54 generating units, 9 tap changing transformers, and 14 shunts VAR compensation devices.

The proposed IHBO is applied on the IEEE 118-bus test system for solving the single-objective and tri-multi objective ORPD problems in this section. The obtained results of optimal variables and considered objective functions are tabulated in Table 7 for cases 15-18. The cases are described as follows:

Case 15: The purpose of this case is to minimize the real power loss using IHBO. The real power loss is 108.2051 MW, where the TVD and VSI are equal to 1.1202 p.u. and 0.1086, respectively.

Case 16: The aim of the case is to minimize the TVD of the system by applying IHBO. The best-minimized value for the TVD is 0.2814 and the values of real power loss and VSI are equal to 138.1058 MW and 0.1707, respectively.

Case 17: The IHBO is implemented here for minimizing the VSI. The minimized value for the VSI is 0.0502. The values of real power loss and TVD are equal to 141.6473 MW and 1.3530 p.u., respectively.
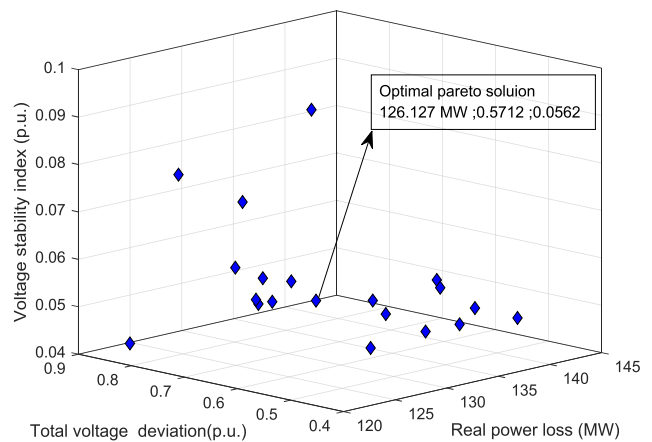

FIGURE 8. Pareto set using IHBO based on multi-objective ORPD (IEEE 118-bus system).

Case 18: The tri-multi objective ORPD problem is solved based on IHBO. The real power loss, TVD, and VSI are minimized simultaneously. Furthermore, the optimal values of the Pareto set are shown in Fig.8. Moreover, the obtained results of minimum values for the real power loss, TVD, and VSI are 126.1271 MW, 0.5712 p.u. and 0.0563, respectively.

The proposed IHBO is also compared with other well-known optimization algorithms and the results are tabulated in Table 8. From this table, it can be observed

TABLE 7. The optimal results obtained using IHBO based on single and tri- multi-objective ORPD problem (IEEE 118-bus system).

Optimal variables	Case 15	Case 16	Case 17	Case 18	Optimal variables Cont.	Case 15	Case 16	Case 17	Case 18
VG1(p.u.)	1.0201	1.0036	0.9895	0.9935	VG90(p.u.)	0.9787	0.9895	1.0000	0.9887
VG4(p.u.)	1.0378	1.0130	0.9764	1.0027	VG91(p.u.)	0.9845	0.9839	1.0124	0.9966
VG6(p.u.)	1.0356	1.0162	0.9790	1.0001	VG92(p.u.)	0.9931	0.9952	1.0083	1.0128
VG8(p.u.)	1.0105	0.9868	1.0091	1.0381	VG99(p.u.)	1.0152	1.0018	0.9975	1.0158
VG10(p.u.)	1.0348	0.9634	0.9714	1.0459	VG100(p.u.)	1.0057	1.0039	1.0009	1.0161
VG12(p.u.)	1.0314	0.9973	0.9831	0.9947	VG103(p.u.)	1.0025	0.9952	1.0187	1.0099
VG15(p.u.)	1.0230	0.9916	1.0008	1.0056	VG104(p.u.)	1.0091	1.0196	1.0210	0.9911
VG18(p.u.)	1.0206	0.9856	0.9966	1.0108	VG105(p.u.)	1.0108	1.0127	1.0205	0.9866
VG19(p.u.)	1.0257	0.9880	1.0041	1.0009	VG107(p.u.)	1.0099	0.9970	1.0400	0.9796
VG24(p.u.)	1.0488	1.0188	1.0545	1.0392	VG110(p.u.)	1.0153	0.9923	1.0174	0.9814
VG25(p.u.)	1.0530	1.0015	1.0402	1.0125	VG111(p.u.)	1.0167	0.9949	1.0177	0.9585
VG26(p.u.)	0.9989	1.0540	1.0493	0.9701	VG112(p.u.)	1.0155	0.9861	1.0103	0.9824
VG27(p.u.)	1.0229	0.9831	1.0370	0.9947	VG113(p.u.)	1.0294	1.0038	1.0172	1.0233
VG31(p.u.)	1.0180	0.9738	1.0261	0.9868	VG116(p.u.)	1.0523	1.0577	1.0576	1.0574
VG32(p.u.)	1.0224	0.9883	1.0380	0.9908	T8(p.u.)	0.9964	0.9520	0.9838	1.0232
VG34(p.u.)	1.0206	1.0082	1.0241	1.0058	T32(p.u.)	0.9503	1.0381	0.9359	0.9989
VG36(p.u.)	1.0186	1.0061	1.0244	1.0056	T36(p.u.)	0.9821	1.0786	1.0850	1.0080
VG40(p.u.)	1.0032	0.9918	0.9976	1.0173	T51(p.u.)	1.0264	1.0779	1.0798	1.0843
VG42(p.u.)	1.0147	0.9817	1.0119	1.0197	T93(p.u.)	0.9620	1.0012	0.9667	1.0077
VG46(p.u.)	1.0000	0.9875	0.9958	0.9832	T95(p.u.)	0.9905	1.0230	1.0912	0.9847
VG49(p.u.)	1.0231	1.0084	1.0047	1.0101	T102(p.u.)	0.9715	0.9881	0.9680	1.0097
VG54(p.u.)	0.9991	1.0275	0.9624	0.9947	T107(p.u.)	0.9223	0.9068	0.9033	0.9018
VG55(p.u.)	1.0052	1.0292	0.9600	0.9898	T127(p.u.)	1.0109	1.0415	1.0513	1.0068
VG56(p.u.)	1.0000	1.0265	0.9596	0.9953	Qc5(MVAR)	5.1013	8.0037	11.1833	9.9526
VG59(p.u.)	1.0335	1.0437	1.0127	1.0210	Qc34(MVAR)	19.4035	19.5427	14.7134	18.7263
VG61(p.u.)	1.0135	1.0283	1.0237	1.0294	Qc37(MVAR)	4.4302	12.1961	15.6696	5.4693
VG62(p.u.)	1.0078	1.0241	1.0174	1.0209	Qc44(MVAR)	11.0657	18.3872	19.7324	3.1684
VG65(p.u.)	1.0500	1.0579	1.0598	1.0526	Qc45(MVAR)	10.6775	11.9349	13.4277	3.0295
VG66(p.u.)	1.0416	1.0400	1.0584	1.0528	Qc46(MVAR)	9.6457	13.2808	7.4969	1.7571
VG69(p.u.)	1.0459	1.0589	1.0580	1.0594	Qc48(MVAR)	0.3006	4.0701	10.9724	9.8931
VG70(p.u.)	0.9881	1.0043	1.0293	1.0313	Qc74(MVAR)	14.7523	12.2376	7.9160	7.8090
VG72(p.u.)	1.0236	1.0043	1.0262	1.0310	Qc79(MVAR)	4.5033	12.0831	17.4251	10.8209
VG73(p.u.)	1.0063	1.0292	1.0267	1.0434	Qc82(MVAR)	6.8231	3.0994	7.5058	18.8280
VG74(p.u.)	0.9975	1.0112	1.0301	1.0217	Qc83(MVAR)	1.9578	14.3909	11.7804	15.6642
VG76(p.u.)	0.9934	1.0112	1.0330	0.9965	Qc105(MVAR)	12.8951	16.4015	11.0329	16.5498
VG77(p.u.)	1.0015	1.0003	1.0169	1.0239	Qc107(MVAR)	13.2690	17.2238	10.2552	12.4595
VG80(p.u.)	0.9935	0.9994	1.0134	1.0285	Qc110(MVAR)	19.9233	6.7481	15.0319	8.1861
VG85(p.u.)	1.0024	0.9835	0.9912	1.0126	Loss	**108.2051**	**138.1058**	**141.6473**	**126.1271**
VG87(p.u.)	1.0114	1.0025	0.9679	1.0198	TVD (p.u.)	**1.1202**	**0.2814**	**1.3530**	**0.5712**
VG89(p.u.)	1.0064	1.0019	1.0179	1.0158	VSI(p.u.)	**0.1086**	**0.1707**	**0.0502**	**0.0563**

TABLE 8. Compared results of single-objective ORPD using different optimization techniques (IEEE 118-bus system).

Methods	OF (s)		
	Minimization of losses	Minimization of TVD	Minimization of VSI
IHBO	108.2051	0.2814	0.0502
HBO	113.2182	0.3729	0.0632
APOPSO	111.8730	0.1980	0.0692
CBA_IV	113.7040	0.3032	0.0570
CBA_III	115.5989	0.3059	0.0587
BA	116.9329	0.3172	0.0613
OGSA	126.9900	0.3666	0.0600
ALC-PSO	121.5300	0.3262	NA
EMA	126.2243	NA	0.4841
QOTLBO	112.2789	0.1910	0.0608
FAHCLPSO	116.2479	0.2218	NA
CLPSO	130.9600	1.6177	0.0965

that the IHBO gives the best minimum values for the three considered objective functions compared with those given by the exchange market algorithm (EMA) [10], APOPSO [38], BA, CBA_III, and CBA_IV [49], FAH-CLPSO [53], ALC-PSO [62],opposition based GSA (OBGSA) [65],quasi-oppositional teaching-learning based

TABLE 9. The best compromise solutions for all studied cases.

Test system	Case #	Type of objective function	Minimized Objective function	P_{loss} (MW)	TVD (p.u.)	VSI (p.u.)
IEEE 30-bus system	Case 1	Single-objective function	Real power loss	**3.4923**	1.4794	3.6435
	Case 2	Single-objective function	Total voltage deviation	4.2417	**0.0854**	1.0658
	Case 3	Single-objective function	Voltage stability index	0.1251	0.2106	**0.0505**
	Case 4	Bi-objective function	Real power loss and total voltage deviation	**3.8842**	**0.2955**	0.2249
	Case 5	Bi-objective function	Real power loss and total voltage stability index	**3.6188**	0.9677	**0.0838**
	Case 6	Bi-objective function	Total voltage deviation and voltage stability index	4.2338	**0.2163**	**0.0583**
	Case 7	Tri-objective function	Real power loss, total voltage deviation and voltage stability index	**3.9254**	**0.3134**	**0.0669**
IEEE 57-bus system	Case 8	Single-objective function	Real power loss	**13.9725**	1.1208	0.8079
	Case 9	Single-objective function	Total voltage deviation	16.4291	**0.8781**	0.8626
	Case 10	Single-objective function	Voltage stability index	19.4196	1.2387	**0.5085**
	Case 11	Bi-objective function	Real power loss and total voltage deviation	**16.0289**	**0.9498**	0.8898
	Case 12	Bi-objective function	Real power loss and total voltage stability index	**15.7423**	1.2133	**0.7798**
	Case 13	Bi-objective function	Total voltage deviation and voltage stability index	21.6997	**1.0744**	**0.6916**
	Case 14	Tri-objective function	Real power loss, total voltage deviation and voltage stability index	**18.1928**	**0.9204**	**0.8152**
IEEE118-bus system	Case 15	Single-objective function	Real power loss	**108.2051**	1.1202	0.1086
	Case 16	Single-objective function	Total voltage deviation	138.1058	**0.2814**	0.1707
	Case 17	Single-objective function	Voltage stability index	141.6473	1.3530	**0.0502**
	Case 18	Tri-objective function	Real power loss, total voltage deviation and voltage stability index	**126.1271**	**0.5712**	**0.0563**

optimization(QOTLBO) [66], and Comprehensive learning PSO (CLPSO) [57].

Finally, Table 9 display the summary of all studied cases over all the three test systems based on the proposed IHB. However, all results of minimized objective functions are showed for single and multi-objective ORPD problem.

VI. CONCLUSION

In this paper, an effective optimization optimizer called IHBO has been proposed to improve the performance of the original HBO which recently published and applied for solving several optimization problems in different fields. In addition, two algorithms based on HBO and IHBO have been developed for solving single and multi-objective ORPD problems. The proposed algorithms have been evaluated and verified on various standards of the IEEE 30-bus, IEEE 57-bus, and IEEE 118-bus test systems. The results confirm high performance

as well as the effectiveness of IHBO in solving the ORPD optimization problems. Furthermore, the coincidence of the optimal obtained results of the large systems like the IEEE 118 bus system validates that the proposed technique overcomes the difficulties related to this type of test system. Also, the results yielded by IHBO have been compared with those obtained by the original HBO along with other available recently meta-heuristics techniques. The simulated results confirm that the IHBO outperforms other compared techniques for solving ORPD in terms of robustness and effectiveness. In the future work, the proposed IHBO could be applied for solving other complex optimization problems in different fields such as optimal distribution generation allocation considering uncertainty of renewable energy resources and load, optimal design and planning of hybrid renewable energy systems, parameter estimation of fuel cells and photovoltaic models.

REFERENCES

[1] L. Dilip, R. Bhesdadiya, I. Trivedi, and P. Jangir, "Optimal power flow problem solution using multi-objective grey wolf optimizer algorithm," in *Intelligent Communication and Computational Technologies*. Springer, 2018, pp. 191–201.

[2] I. N. Trivedi, P. Jangir, S. A. Parmar, and N. Jangir, "Optimal power flow with voltage stability improvement and loss reduction in power system using moth-flame optimizer," *Neural Comput. Appl.*, vol. 30, no. 6, pp. 1889–1904, Sep. 2018.

[3] I. N. Trivedi, P. Jangir, and S. A. Parmar, "Optimal power flow with enhancement of voltage stability and reduction of power loss using ant-lion optimizer," *Cogent Eng.*, vol. 3, no. 1, Dec. 2016, Art. no. 1208942.

[4] S. S. Reddy, "Multi-objective optimization considering cost, emission and loss objectives using PSO and fuzzy approach," *Int. J. Eng. Technol.*, vol. 7, no. 3, pp. 1552–1557, 2018.

[5] A. K. Das, R. Majumdar, B. k. Panigrahi, and S. S. Reddy, "Optimal power flow for Indian 75 bus system using differential evolution," in *Swarm, Evolutionary, and Memetic Computing* (Lecture Notes in Computer Science), vol. 7076, B. K. Panigrahi, P. N. Suganthan, S. Das, and S. C. Satapathy, Eds. Berlin, Germany: Springer, 2011.

[6] S. S. Reddy, "Multi-objective optimal power flow for a thermal-wind-solar power system," *J. Green Eng.*, vol. 7, no. 4, pp. 451–476, 2017.

[7] B. Bentouati, S. Chettih, P. Jangir, and I. N. Trivedi, "A solution to the optimal power flow using multi-verse optimizer," *J. Electr. Syst.*, vol. 12, no. 4, pp. 1–18, 2016.

[8] R. H. Bhesdadiya, I. N. Trivedi, P. Jangir, N. Jangir, and A. Kumar, "An NSGA-III algorithm for solving multi-objective economic/environmental dispatch problem," *Cogent Eng.*, vol. 3, no. 1, Dec. 2016, Art. no. 1269383.

[9] J. Radosavljevic, *Metaheuristic Optimization in Power Engineering*. London, U.K.: Institution Engineering Technology (IET), 2018.

[10] A. Rajan and T. Malakar, "Exchange market algorithm based optimum reactive power dispatch," *Appl. Soft Comput.*, vol. 43, pp. 320–336, Jun. 2016.

[11] P. Jangir, S. A. Parmar, I. N. Trivedi, and R. H. Bhesdadiya, "A novel hybrid particle swarm optimizer with multi verse optimizer for global numerical optimization and optimal reactive power dispatch problem," *Eng. Sci. Technol., Int. J.*, vol. 20, no. 2, pp. 570–586, Apr. 2017.

[12] J. Radosavljevic, M. Jevtic, and M. Milovanovic, "A solution to the ORPD problem and critical analysis of the results," *Electr. Eng.*, vol. 100, no. 1, pp. 253–265, Mar. 2018, doi: 10.1007/s00202-016-0503-1.

[13] N. I. Deeb and S. M. Shahidehpour, "An efficient technique for reactive power dispatch using a revised linear programming approach," *Electr. Power Syst. Res.*, vol. 15, no. 2, pp. 121–134, Oct. 1988.

[14] D. S. Kirschen and H. P. Van Meeteren, "MW/voltage control in a linear programming based optimal power flow," *IEEE Trans. Power Syst.*, vol. 3, no. 2, pp. 481–489, May 1988.

[15] W. Yan, J. Yu, D. C. Yu, and K. Bhattarai, "A new optimal reactive power flow model in rectangular form and its solution by predictor corrector primal dual interior point method," *IEEE Trans. Power Syst.*, vol. 21, no. 1, pp. 61–67, Feb. 2006.

[16] J. Z. Zhu and X. F. Xiong, "Optimal reactive power control using modified interior point method," *Electr. Power Syst. Res.*, vol. 66, no. 2, pp. 187–192, Aug. 2003.

[17] N. Deeb and S. M. Shahidehpour, "Linear reactive power optimization in a large power network using the decomposition approach," *IEEE Trans. Power Syst.*, vol. 5, no. 2, pp. 428–438, May 1990.

[18] S. Mirjalili, S. M. Mirjalili, and A. Lewis, "Grey wolf optimizer," *Adv. Eng. Softw.*, vol. 69, pp. 46–61, Mar. 2014.

[19] H. Buch, I. N. Trivedi, and P. Jangir, "Moth flame optimization to solve optimal power flow with non-parametric statistical evaluation validation," *Cogent Eng.*, vol. 4, no. 1, Jan. 2017, Art. no. 1286731.

[20] M. Premkumar, P. Jangir, R. Sowmya, H. H. Alhelou, A. A. Heidari, and H. Chen, "MOSMA: Multi-objective slime Mould algorithm based on elitist non-dominated sorting," *IEEE Access*, vol. 9, pp. 3229–3248, 2021.

[21] S. Mirjalili, P. Jangir, and S. Saremi, "Multi-objective ant lion optimizer: A multi-objective optimization algorithm for solving engineering problems," *Appl. Intell.*, vol. 46, no. 1, pp. 79–95, 2017.

[22] A. A. A. El-Ela, M. A. Abido, and S. R. Spea, "Diferential evolution algortihm for optimal reactive power dispatch," *Electr. Power Syst. Res.*, vol. 81, no. 2, pp. 458–464, 2011.

[23] W. S. Sakr, R. A. EL-Sehiemy, and A. M. Azmy, "Adaptive differential evolution algorithm for efficient reactive power management," *Appl. Soft Comput.*, vol. 53, pp. 336–351, Apr. 2017.

[24] K. Abaci and V. Yamacli, "Optimal reactive-power dispatch using differential search algorithm," *Elect. Eng.*, vol. 99, pp. 213–225, Aug. 2016, doi: 10.1007/s00202-016-0410-5.

[25] S. Duman, Y. Sonmez, U. Guvenc, and N. Yorukeren, "Optimal reactive power dispatch using a gravitational search algorithm," *IET Gener., Transmiss. Distrib.*, vol. 6, no. 6, pp. 563–576, Jun. 2012.

[26] M. H. Sulaiman, Z. Mustaffa, M. R. Mohamed, and O. Aliman, "Using the gray wolf optimizer for solving optimal reactive power dispatch problem," *Appl. Soft Comput.*, vol. 32, pp. 286–292, Jul. 2015.

[27] S. Dutta, P. Mukhopadhyay, P. K. Roy, and D. Nandi, "Unified power flow controller based reactive power dispatch using oppositional krill herd algorithm," *Int. J. Electr. Power Energy Syst.*, vol. 80, pp. 10–25, Sep. 2016.

[28] M. H. Sulaiman and Z. Mustaffa, "Cuckoo search algorithm as an optimizer for optimal reactive power dispatch problems," in *Proc. 3rd Int. Conf. Control, Autom. Robot. (ICCAR)*, Apr. 2017, pp. 735–739.

[29] S. Mouassa, T. Bouktir, and A. Salhi, "Ant lion optimizer for solving optimal reactive power dispatch problem in power systems," *Eng. Sci. Technol., Int. J.*, vol. 20, no. 3, pp. 885–895, Jun. 2017.

[30] E. Agbugba, "Hybridization of particle swarm optimization with bat algorithm for optimal reactive power dispatch," M.S. thesis, Dept. Electr. Eng., Univ. South Africa, Pretoria, South Africa, Jun. 2017.

[31] M. S. Saddique, A. R. Bhatti, S. S. Haroon, M. K. Sattar, S. Amin, I. A. Sajjad, S. S. ul Haq, A. B. Awan, and N. Rasheed, "Solution to optimal reactive power dispatch in transmission system using meta-heuristic techniques—Status and technological review," *Electr. Power Syst. Res.*, vol. 178, Jan. 2020, Art. no. 106031.

[32] M. W. Khan, Y. Muhammad, M. A. Z. Raja, F. Ullah, N. I. Chaudhary, and Y. He, "A new fractional particle swarm optimization with entropy diversity based velocity for reactive power planning," *Entropy*, vol. 22, no. 10, p. 1112, Oct. 2020.

[33] M. Ghasemi, M. M. Ghanbarian, S. Ghavidel, S. Rahmani, and M. E. Mahboubi, "Modified teaching learning algorithm and double differential evolution algorithm for optimal reactive power dispatch problem: A comparative study," *Inf. Sci.*, vol. 278, pp. 231–249, Sep. 2014.

[34] A. Rajan and T. Malakar, "Optimal reactive power dispatch using hybrid Nelder–Mead simplex based firefly algorithm," *Elect. Power Energy Syst.*, vol. 66, pp. 9–24, Mar. 2015.

[35] M. Ghasemi, S. Ghavidel, M. M. Ghanbarian, and A. Habibi, "A new hybrid algorithm for optimal reactive power dispatch problem with discrete and continuous control variables," *Appl. Soft Comput.*, vol. 22, pp. 126–140, Sep. 2014.

[36] M. Mehdinejad, B. Mohammadi-Ivatloo, R. Dadashzadeh-Bonab, and K. Zare, "Solution of optimal reactive power dispatch of power systems using hybrid particle swarm optimization and imperialist competitive algorithms," *Elect. Power Energy Syst.*, vol. 83, pp. 104–116, Dec. 2016.

[37] Y. Li, X. Li, and Z. Li, "Reactive power optimization using hybrid CABC-DE algorithm," *Electr. Power Compon. Syst.*, vol. 45, no. 9, pp. 980–989, May 2017.

[38] T. M. Aljohani, A. F. Ebrahim, and O. Mohammed, "Single and multiobjective optimal reactive power dispatch based on hybrid artificial physics–particle swarm optimization," *Electr. Power Compon. Syst.* vol. 12, no. 12, pp. 1–24, 2019.

[39] S. Mirjalili, P. Jangir, S. Z. Mirjalili, S. Saremi, and I. N. Trivedi, "Optimization of problems with multiple objectives using the multi-verse optimization algorithm," *Knowl.-Based Syst.*, vol. 134, pp. 50–71, Oct. 2017.

[40] P. Jangir and N. Jangir, "A new non-dominated sorting grey wolf optimizer (NS-GWO) algorithm: Development and application to solve engineering designs and economic constrained emission dispatch problem with integration of wind power," *Eng. Appl. Artif. Intell.*, vol. 72, pp. 449–467, Jun. 2018.

[41] G. Kaur and S. Arora, "Chaotic whale optimization algorithm," *J. Comput. Des. Eng.*, vol. 5, no. 3, pp. 275–284, Jul. 2018.

[42] S. Mirjalili and A. H. Gandomi, "Chaotic gravitational constants for the gravitational search algorithm," *Appl. Soft Comput.*, vol. 53, pp. 407–419, Apr. 2017.

[43] M. Kohli and S. Arora, "Chaotic grey wolf optimization algorithm for constrained optimization problems," *J. Comput. Des. Eng.*, vol. 5, no. 4, pp. 458–472, Oct. 2018.

[44] S. Arora and S. Singh, "An improved butterfly optimization algorithm with chaos," *J. Intell. Fuzzy Syst.*, vol. 32, no. 1, pp. 1079–1088, Jan. 2017.

[45] Q. Zhang, H. Chen, A. A. Heidari, X. Zhao, Y. Xu, P. Wang, Y. Li, and C. Li, "Chaos-induced and mutation-driven schemes boosting salp chains-inspired optimizers," *IEEE Access*, vol. 7, pp. 31243–31261, 2019.

[46] Y. Xu, H. Chen, A. A. Heidari, J. Luo, Q. Zhang, X. Zhao, and C. Li, "An efficient chaotic mutative moth-flame-inspired optimizer for global optimization tasks," *Expert Syst. Appl.*, vol. 129, pp. 135–155, Sep. 2019.

[47] A. Mukherjee and V. Mukherjee, "Chaotic krill herd algorithm for optimal reactive power dispatch considering FACTS devices," *Appl. Soft Comput.*, vol. 44, pp. 163–190, Jul. 2016.

[48] A. Mukherjee and V. Mukherjee, "Chaos embedded krill herd algorithm for optimal VAR dispatch problem of power system," *Int. J. Electr. Power Energy Syst.*, vol. 82, pp. 37–48, Nov. 2016.

[49] S. Mugemanyi, Z. Qu, F. X. Rugema, Y. Dong, C. Bananeza, and L. Wang, "Optimal reactive power dispatch using chaotic bat algorithm," *IEEE Access*, vol. 8, pp. 65830–65867, 2020.

[50] M. Abido and J. Bakhashwain, "Optimal VAR dispatch using a multiobjective evolutionary algorithm," *Int. J. Electr. Power Energy Syst.*, vol. 27, pp. 13–20, Jan. 2005.

[51] G. Chen, L. Liu, P. Song, and Y. Du, "Chaotic improved PSO-based multi-objective optimization for minimization of power losses and L index in power systems," *Energy Convers. Manage.*, vol. 86, pp. 548–560, Oct. 2014.

[52] B. B. Pal, P. Biswas, and A. Mukhopadhyay, "GA based FGP approach for optimal reactive power dispatch," *Procedia Technol.*, vol. 10, pp. 464–473, 2013.

[53] E. Naderi, H. Narimani, M. Fathi, and M. R. Narimani, "A novel fuzzy adaptive configuration of particle swarm optimization to solve large-scale optimal reactive power dispatch," *Appl. Soft Comput.*, vol. 53, pp. 441–456, Apr. 2017.

[54] E. E. Elattar and S. ElSayed, "Modified JAYA algorithm for optimal power flow incorporating renewable energy sources considering the cost, emission, power loss and voltage profile improvement," *Energy*, vol. 178, pp. 598–609, Jul. 2019.

[55] Q. Askari, M. Saeed, and I. Younas, "Heap-based optimizer inspired by corporate rank hierarchy for global optimization," *Expert Syst. Appl.*, vol. 161, Dec. 2020, Art. no. 113702.

[56] K. Ayan and U. Kılıç, "Artificial bee colony algorithm solution for optimal reactive power flow," *Appl. Soft Comput.*, vol. 12, pp. 1477–1482, May 2012.

[57] K. Mahadevan and P. S. Kannan, "Comprehensive learning particle swarm optimization for reactive power dispatch," *Appl. Soft Comput.*, vol. 10, pp. 641–652, Mar. 2010.

[58] A. Mukherjee and V. Mukherjee, "Solution of optimal reactive power dispatch by chaotic krill herd algorithm," *IET Gener., Transmiss. Distrib.*, vol. 9, no. 15, pp. 2351–2362, 2015.

[59] Illinois Center for a Smarter Electric Grid (ICSEG). *The IEEE 57-Bus Test System.* Accessed: Dec. 25, 2020. [Online]. Available: https://icseg.iti.illinois.edu/ieee-57-bus-system/

[60] C. Dai, W. Chen, Y. Zhu, and X. Zhang, "Seeker optimization algorithm for optimal reactive power dispatch," *IEEE Trans. Power Syst.*, vol. 24, no. 3, pp. 1218–1231, Aug. 2009.

[61] M. R. Nayak, K. R. Krishnanand, and P. K. Rout, "Optimal reactive power dispatch based on adaptive invasive weed optimization algorithm," in *Proc. Int. Conf. Energy, Autom. Signal*, Dec. 2011, pp. 1–7.

[62] R. P. Singh, V. Mukherjee, and S. P. Ghoshal, "Optimal reactive power dispatch by particle swarm optimization with an aging leader and challengers," *Appl. Soft Comput.*, vol. 29, pp. 298–309, Apr. 2015.

[63] R. Mallipeddi, S. Jeyadevi, P. N. Suganthan, and S. Baskar, "Efficient constraint handling for optimal reactive power dispatch problems," *Swarm Evol. Comput.*, vol. 5, pp. 28–36, Aug. 2012.

[64] *The IEEE 118-Bus Test System.* Accessed: Dec. 25, 2020. [Online]. Available: http://labs.ece.uw.edu/pstca/pf118/pg_tca118bus.htm

[65] B. Shaw, V. Mukherjee, and S. P. Ghoshal, "Solution of reactive power dispatch of power systems by an opposition-based gravitational search algorithm," *Int. J. Electr. Power Energy Syst.*, vol. 55, pp. 29–40, Feb. 2014.

[66] B. Mandal and P. K. Roy, "Optimal reactive power dispatch using quasi-oppositional teaching learning based optimization," *Int. J. Electr. Power Energy Syst.*, vol. 53, pp. 123–134, Dec. 2013.

SALAH K. ELSAYED received the B.Sc. and Ph.D. degrees from the Department of Electrical Power and Machines, Faculty of Engineering, Al-Azhar University, Egypt, in 2009 and 2012, respectively. In 2012, he joined the Faculty of Engineering, Al-Azhar University, as a Lecturer, where he is currently working as an Associate Professor with the Department of Electrical Power and Machines. His research interests include power system stability and control, optimization of power systems, renewable energy applications in power system applications of AI and metaheuristic optimization techniques for solving electrical power system problems, energy management, microgrid, optimization, and smart grids.

SALAH KAMEL received the International Ph.D. degree from the University of Jaen, Spain (Main) and Aalborg University, Denmark (Host), in January 2014. He is currently an Associate Professor with the Electrical Engineering Department, Aswan University. He is also a Leader of the Power Systems Research Group, Advanced Power Systems Research Laboratory (APSR Lab), Aswan, Egypt. His research interests include power system analysis and optimization, smart grid, and renewable energy systems.

ALI SELIM received the B.Sc. and M.Sc. degrees in electrical engineering from Aswan University, Aswan, Egypt, in 2010 and 2016, respectively, and the Ph.D. degree in electrical engineering from the University of Jaén, Spain, in 2020. He is currently an Assistant Professor with the Electrical Engineering Department, Aswan University. His research interests include mathematical optimization, planning, and control of power systems, renewable energies, energy storage, and smart grids.

MAHROUS AHMED (Senior Member, IEEE) received the B.S. and M.Sc. degrees in electrical engineering from Assiut University, Assiut, Egypt, in 1996 and 2000, respectively, and the Ph.D. degree in electrical engineering from the University of Malaya, Kuala Lumpur, Malaysia, in 2007. Since 2007, he has been an Assistant Professor with the Faculty of Engineering, Aswan University, Aswan, Egypt, where he became an Associate Professor, in 2014. He has been a Professor with the Faculty of Engineering, Aswan University, since 2019. He is currently an Associate Professor with the Faculty of Engineering, Taif University, Saudi Arabia. He has published more than 70 papers in an international sited journals and conferences. His research interests include power conversion topologies and techniques, real time control, renewable energy systems, and power electronics applications. He has awarded more than ten research funded projects in the field of power electronics applications.

● ● ●